Observational evidence for westward propagation of temperature inversions in the southeastern Arabian Sea

D. Shankar,[1] V. V. Gopalakrishna,[1] S. S. C. Shenoi,[1] F. Durand,[1] S. R. Shetye,[1]
C. K. Rajan,[2] Z. Johnson,[2] N. Araligidad[1], and G. S. Michael[1]

A warm pool forms in the southeastern Arabian Sea (SEAS) prior to the onset of the summer monsoon over India in early June; the core of this warm pool is in the Lakshadweep Sea (LS). XBT and surface salinity data collected in the LS during May-2002–April-2003 show that temperature inversions occur off the southwest coast of India in early December with the arrival of low-salinity waters from the Bay of Bengal. The low-salinity waters and the inversions propagate westward along with the downwelling Rossby waves that constitute the Lakshadweep sea-level high; inversions occur in the western LS ($\sim 73^\circ$E) about 40 days after they occur near the coast in the eastern LS ($\sim 75.5^\circ$E). They disappear in April, when the Tropical Convergence Zone moves over the SEAS and the warm pool engulfs the region. Ocean dynamics and air-sea fluxes are together responsible for the formation and westward propagation of the inversions.

1. Introduction

Prior to the onset of the summer monsoon over India in late May or early June, a huge warm pool, with sea surface temperature (SST) greater than 28°C, covers the north Indian Ocean, making it among the warmest regions in the world oceans [*Joseph*, 1990; *Vinayachandran and Shetye*, 1991; *Rao and Sivakumar*, 1999]. In the Arabian Sea, the core of this warm pool lies in the Lakshadweep Sea (LS) [*Shenoi et al.*, 1999], the part of the southeastern Arabian Sea (SEAS) that lies between the Indian peninsula and the Lakshadweep islands to its west (Figure 1). *Shenoi et al.* [1999] showed that an SST high (SSTH) develops in the LS in February–March, well before the large-scale warming that occurs later in the SEAS. They argued that the SSTH is intimately connected to the sea-level high, called Lakshadweep high (LH) [*Bruce et al.*, 1994; *Shankar and Shetye*, 1997; *Bruce et al.*, 1998], that forms in the SEAS during December. Low-salinity waters from the northern Bay of Bengal are brought into the LS early during November–January (see schematic in Figure 2) [*Shetye et al.*, 1991; *Rao and Sivakumar*, 2003; *Han and McCreary*, 2001; *Han et al.*, 2001; *Schott and McCreary*, 2001]. *Shenoi et al.* [1999] argued that the low surface salinity and the downwelling associated with the LH [*Bruce et al.*, 1994; *Shankar and Shetye*, 1997] stabilize the surface layer and provide a breeding ground for the formation of the SSTH.

Climatological data from the SEAS have shown the existence of a "barrier layer" below the low-salinity surface mixed layer [*Sprintall and Tomczak*, 1992; *Rao and Sivakumar*, 2003]. An analysis of available Bathy Thermograph (BT) profiles also showed the presence of temperature inversions below the mixed layer during the winter monsoon [*Thadathil and Gosh*, 1992]. Model simulations show that these inversions form in the barrier layer and they heat the surface layer above, contributing to a 1.1°C increase in SST during November–March, when the atmospheric fluxes cool the surface by 0.3°C [*Durand et al.*, 2004]. This implies that the ocean plays an active role in the formation of the SSTH, unlike the passive role envisaged by *Shenoi et al.* [1999]. By March, owing to the increase in solar insolation due to the northward march of the Sun [*Sengupta et al.*, 2002] and the deep, stable surface layer, the SSTH reaches a mature phase in the LS. Even in May, when the Tropical Convergence Zone moves over the region and it is engulfed by the warm pool, the SSTH retains its identity within the warm pool [*Shenoi et al.*, 1999].

The onset of the summer monsoon over India is often, but not always, accompanied by the formation of an "onset vortex" [*Krishnamurti et al.*, 1981] in the SEAS, and this suggests a possible link between it and the warm SEAS [*Joseph*, 1990; *Rao and Sivakumar*, 1999; *Shenoi et al.*, 1999]. *Shenoi et al.* [1999] speculated that by maintaining SST higher than 28°C, a rough threshold for deep atmospheric convection in the monsoon region [*Gadgil et al.*, 1984], the SSTH in the LS and the warm pool in the SEAS satisfied a condition necessary, though not sufficient, for the formation of the onset vortex.

The evolution of the SSTH in the LS and its possible role in the process of monsoon onset was investigated recently under the Arabian Sea Monsoon Experiment (ARMEX), a field experiment under the Indian Climate Research Programme. As part of ARMEX, twice-monthly Expendable Bathy Thermograph (XBT) surveys were conducted during May-2002–April-2003 using feeder ships plying between Kochi on the Indian mainland and the Lakshadweep islands (Figure 1). 7–13 XBTs were deployed during each survey and samples of surface water were collected with each deployment for subsequent salinity analysis. The XBT data analysed by *Thadathil and Gosh* [1992] were sufficient only for proving the existence of inversions. In this paper, we use XBT data from the ARMEX surveys in conjunction with model simulations [*Durand et al.*, 2004] to describe the spatio-temporal evolution of temperature inversions in the LS. The model used is the OPA OGCM [*Madec et al.*, 1996] applied to the global ocean with 0.5° horizontal resolution and vertical resolution of 10 m in the top 120 m. It was forced by the seasonal climatology of ERS1-2 winds [*Bentamy et al.*, 1996] and CMAP precipitation flux [*Xie and Arkin*, 1996]. The heat fluxes were diagnosed from the NCEP/NCAR Reanalyses [*Kalnay et al.*, 1996] temperature.

2. Evolution of inversions

We consider a profile to have an inversion if the sub-surface temperature exceeds SST by at least 0.25°C. The temporal variation of inversions in the LS is shown in Figure 3a. Inversions are first observed late in October, when about 10% of the profiles show inversions. After a decline in November, the percentage of profiles with inversions starts increasing in December; by early February, almost 85% of the profiles show inversions. Inversions start declining by early March, when SST increases [*Shenoi et al.*, 1999]. The number of inversions increases again in April, but these are extremely shallow and occur close to the surface. With the onset of the summer monsoon, inversions once again decline in the LS.

[1]National Institute of Oceanography, Goa, India.
[2]Cochin University of Science and Technology, Kochi, India.

0094-8276/06/$5.00

There is considerable difference even within the LS in the temporal evolution of inversions; inversions occur first in the eastern and southern LS, then in the west. A time-longitude plot of the occurrence of inversions on the best-sampled track, which runs between Kochi and the northern Lakshadweep islands (Figure 1), shows that the lag is about 30–40 days; inversions occur at 76°E in mid-December and at 72°E in mid-January (Figure 3b,c). They also disappear a little earlier in the east than in the west, but the lag is less than 15 days for the collapse of inversions. The observed westward migration of inversions matches that seen in the climatological numerical simulation of [*Durand et al.*, 2004] (Figure 3b,c). There is, however, an apparent shift in phase, the strongest inversion in the model appearing in December–January and that in the observations during January–February. There are two possible reasons for the discrepancy. First, the model does not include the diurnal cycle, and all the observations in the eastern LS during the period of inversions were made during the afternoon (owing to logistical reasons). Second, there are likely to be differences between a climatological simulation and observations for a particular year. The data and simulations are insufficient to permit a more detailed analysis to separate these two effects.

To show the evolution of vertical structure, we construct a time series for two circles near the ends of best-sampled track (Figure 1); temperature profiles available within these circles are considered to be representative of the circle and are stacked together in a time series for each circle (Figure 3d,e). Inversions occur in the east in early December, about 40 days before they occur in the west (mid-January). The inversions decline with the increase in SST by early March, but the increase in surface temperature does not extend to the depth of the inversion layer; the sub-surface temperature maximum is less than SST, but higher than the temperature above it (the maximum), leading to a "sub-surface inversion" (Figure 3d,e). Even these decline later in April. The occurrence of the winter-monsoon salinity minimum in the west also lags that in the east (Figure 3f), as in the climatological model simulation (Figure 3c). Thus, both data and models show that the salinity minimum and temperature inversions migrate westward across the LS during November–February.

3. Discussion

Salinity decreases in the LS during the winter monsoon because of inflow of low-salinity waters from the northern bay [*Shetye et al.*, 1991]. The lowest salinities south of India occur in November [*Shankar*, 2000; *Han and McCreary*, 2001], when the equatorward East India Coastal Current (EICC) carries the low-salinity waters from the northern bay into the Winter Monsoon Current (WMC), which, in turn, flows into the poleward West India Coastal Current (WICC) in November [*Shankar et al.*, 2002] (Figure 2). Hence, the salinity of the WMC increases with time; therefore, the low-salinity waters transported by it to the northwestern LS are more saline than those transported to the eastern LS (Figure 3c,f). Model studies show that these currents are associated with a downwelling Kelvin wave triggered along the Indian east coast with the collapse of the summer monsoon [*McCreary et al.*, 1993, 1996; *Shankar et al.*, 2002]. The Kelvin wave turns around Sri Lanka to propagate poleward along the Indian west coast, radiating a westward propagating Rossby wave in the process. As the Rossby wave radiates offshore from the Indian west coast, the WMC migrates westward with it and the LH forms [*Shankar and Shetye*, 1997] (Figure 2). The WMC bifurcates in the SEAS, one arm flowing due west, the other flowing around the LH as its western arm and the front of the Rossby wave [*Shankar et al.*, 2002]. Hence, salinity decreases earlier in the south and east, then in the northwest of the LS (Figure 3c,f). The propagation speed is about 10 cm s^{-1} (Figure 3b,c), comparable to the speed estimated for annual Rossby waves from altimeter and hydrographic observations farther east [*Brandt et al.*, 2002], and it appears as a second-baroclinic-mode wave in the model. Hence, the ARMEX data presented above suggest that the barrier layer and the temperature inversions in this layer migrate westward along with the Rossby waves that constitute the LH.

One possible cause of the inversions is the barrier-layer mechanism, i.e., loss of incoming shortwave radiation to the barrier or inversion layer through the bottom of the surface mixed layer in the LS [*Vialard and Delecluse*, 1998]. Another reason is that the low-salinity waters entering the LS are cooled at the surface en route to the LS [*Thadathil and Gosh*, 1992] owing to a net heat flux out of the ocean (Figure 2). Cooling of these waters occurs largely in the southern Bay of Bengal during November–December owing to a sharp decrease in the net shortwave radiation [*Hastenrath and Lamb*, 1991; *Josey et al.*, 1996]. These waters are also cooled off the southern tip of India, where the latent heat flux increases sharply in January owing to the channeling of the winter monsoon winds between India and Sri Lanka [*Luis and Kawamura*, 2000]. This surface cooling is strongest during the winter monsoon.

The inversions decline with the increase in surface heating in March, when the SSTH forms in the LS. In contrast to the inversions observed in the LS during the winter monsoon, the shallow inversions that occur during April (Figure 3d,e), by when the warm pool covers the SEAS, are likely to be a result of cooling at night. Inversions during this period are not seen during the day, but the data are not sufficient to permit an analysis of such diurnal variations in the temperature inversions.

In conclusion, we have shown that just as the LH and SSTH in the LS propagate westward as a consequence of the radiation of westward propagating Rossby waves, the low-salinity waters that are carried into the region by the WMC also migrate westward. Air-sea fluxes cool the near-surface regime of the low-salinity waters. A barrier layer supports the cooling, leading to the formation of temperature inversions, which also migrate westward. CTD time-series observations during ARMEX show that the barrier layer in the LS is annihilated in May by upwelling and the inflow of high-salinity waters from the north [*Shenoi et al.*, 2004]. Like the Kelvin and Rossby waves that force the LH, the upwelling in the LS, which leads to the formation of the Lakshadweep Low during the summer monsoon [*Shankar and Shetye*, 1997], and the equatorward WICC that brings in the high-salinity waters from the northern Arabian Sea, are largely due to remote forcing from the Bay of Bengal [*Shenoi et al.*, 2004]. The formation, westward propagation, and eventual annihilation of the barrier layer in the LS are thus a consequence of ocean dynamics and near-surface thermodynamics involving air-sea fluxes.

Acknowledgments. We thank the master and crew of M. V. Tipu Sultan and M. V. Bharat Seema for their assistance during the XBT surveys, Jérôme Vialard for useful discussions, and R. Uchil for Figures 2 and 3. This work was supported by DST (under ARMEX) and DOD, India. FD was funded by the Indo-French Center for Environment and Climate. This is NIO contribution 3879.

References

Bentamy, A., Y. Quilfen, F. Gohin, N. Grima, M. Lenaour, and J. Servain, Determination and validation of average wind fi elds from ERS-1 scatterometer measurements, *Global Atmos. Ocean. Syst.*, *4*, 1–29, 1996.

Brandt, P., L. Stramma, F. Schott, J. Fischer, M. Dengler, and D. Quadfasel, Annual Rossby waves in the Arabian Sea from TOPEX/Poseidon altimeter and in situ data, *Deep-Sea Res. II*, *49*, 1197–1210, 2002.

Bruce, J. G., D. R. Johnson, and J. C. Kindle, Evidence for eddy formation in the eastern Arabian Sea during the northeast monsoon, *J. Geophys. Res.*, *99*, 7651–7664, 1994.

Bruce, J. G., J. C. Kindle, L. H. Kantha, J. L. Kerling, and J. F. Bailey, Recent observations and modeling in the Arabian Sea Laccadive High region, *J. Geophys. Res.*, *103*, 7593–7600, 1998.

Durand, F., S. R. Shetye, J. Vialard, D. Shankar, S. S. C. Shenoi, C. Ethe, and G. Madec, Impact of temperature inversions on SST evolution in the southeastern Arabian Sea during the pre-summer monsoon season, *Geophys. Res. Lett.*, *31*, L01305, doi:10.1029/2003GL018906, 2004.

Gadgil, S., P. Joseph, and N. Joshi, Ocean-atmosphere coupling over monsoon regions, *Nature*, *312*, 141–143, 1984.

Han, W., and J. P. McCreary, Modeling salinity distributions in the Indian Ocean, *J. Geophys. Res.*, *106*, 859–877, 2001.

Han, W., J. P. McCreary, and K. Kohler, Influence of precipitation minus evaporation and Bay of Bengal rivers on dynamics, thermodynamics, and mixed-layer physics in the upper Indian Ocean, *J. Geophys. Res.*, *106*, 6895–6916, 2001.

Hastenrath, S., and P. Lamb, Climatic atlas of the Indian Ocean, Part II: Heat budget, *Tech. rep.*, University of Wisconsin, Madison, 1991.

Joseph, P. V., Warm pool over the Indian Ocean and monsoon onset, *Tropical Ocean and Atmosphere Newsletter*, *53*, 1–5, 1990.

Josey, S. A., E. C. Kent, D. Oakley, and P. K. Taylor, A new global air–sea heat and momentum flux climatology, *International WOCE Newsletter*, *24*, 3–5, 1996.

Kalnay, E., et al., The NCEP/NCAR 40-year reanalysis project, *Bull. Am. Meteorol. Soc.*, *77*, 437–471, 1996.

Krishnamurti, T. N., P. A. Y. Ramanathan, and R. Pasch, On the onset vortex of the summer monsoon, *Mon. Wea. Rev.*, *109*, 344–363, 1981.

Luis, A. J., and H. Kawamura, Wintertime wind forcing and sea surface cooling near the south India tip observed using NSCAT and AVHRR, *Rem. Sens. Environ.*, *73*, 55–64, 2000.

Madec, G., P. Delecluse, M. Imbard, and C. Levy, *OPA 8.1 Ocean General Circulation Model reference manual*, Note du Pole de modélisation, Institut Pierre Simon Laplace (IPSL), France, 1996.

McCreary, J. P., P. K. Kundu, and R. L. Molinari, A numerical investigation of the dynamics, thermodynamics and mixed-layer processes in the Indian Ocean, *Prog. Oceanogr.*, *31*, 181–244, 1993.

McCreary, J. P., W. Han, D. Shankar, and S. R. Shetye, Dynamics of the East India Coastal Current, 2. Numerical solutions, *J. Geophys. Res.*, *101*, 13,993–14,010, 1996.

Rao, R. R., and R. Sivakumar, On the possible mechanisms of the evolution of a mini-warm pool during the pre-summer monsoon season and the onset vortex in the southeastern Arabian Sea, *Q. J. R. Met. Soc.*, *125*, 787–809, 1999.

Rao, R. R., and R. Sivakumar, Seasonal variability of sea surface salinity and salt budget of the mixed layer of the north Indian Ocean, *J. Geophys. Res.*, *108*, 3009, doi:10.1029/2001JC000907, 2003.

Schott, F., and J. P. McCreary, The monsoon circulation in the Indian Ocean, *Progr. Oceanogr.*, *51*, 1–123, 2001.

Sengupta, D., P. K. Ray, and G. S. Bhat, Spring warming of the eastern Arabian Sea and Bay of Bengal from buoy data, *Geophys. Res. Lett.*, *29*, doi:10.1029/2002GL015340, 2002.

Shankar, D., Seasonal cycle of sea level and currents along the coast of India, *Curr. Sci.*, *78*, 279–288, 2000.

Shankar, D., and S. R. Shetye, On the dynamics of the Lakshadweep high and low in the southeastern Arabian Sea, *J. Geophys. Res.*, *102*, 12,551–12,562, 1997.

Shankar, D., P. N. Vinayachandran, and A. S. Unnikrishnan, The monsoon currents in the north Indian Ocean, *Progr. Oceanogr.*, *52*, 63–120, 2002.

Shenoi, S. S. C., D. Shankar, and S. R. Shetye, On the sea surface temperature high in the Lakshadweep Sea before the onset of the southwest monsoon, *J. Geophys. Res.*, *104*, 15,703–15,712, 1999.

Shenoi, S. S. C., D. Shankar, and S. R. Shetye, Remote forcing annihilates barrier layer in southeastern Arabian Sea, *Geophys. Res. Lett.*, L05307, doi:10.1029/2003GL019270, 2004.

Shetye, S. R., A. D. Gouveia, S. S. C. Shenoi, G. S. Michael, D. Sundar, A. M. Almeida, and K. Santanam, The coastal current off western India during the northeast monsoon, *Deep-Sea Research*, *38*, 1517–1529, 1991.

Sprintall, J., and M. Tomczak, Evidence of the barrier layer in the surface layer of the tropics, *J. Geophys. Res.*, *97*, 7305–7316, 1992.

Thadathil, P., and A. Gosh, Surface layer temperature inversion in the Arabian Sea during winter, *J. Oceanogr.*, *48*, 293–304, 1992.

Vialard, J., and P. Delecluse, An OGCM study for the TOGA decade. Part II: Barrier-layer formation and variability, *J. Phys. Oceanogr.*, *28*, 1089–1106, 1998.

Vinayachandran, P. N., and S. R. Shetye, The warm pool in the Indian Ocean, *Proc. Ind. Acad. Sci.(Earth Planet. Sci.)*, *100*, 165–175, 1991.

Xie, P., and P. Arkin, Analyses of global monthly precipitation using gauge observations, satellite estimates, and numerical model predictions, *J. Clim.*, *9*, 840–858, 1996.

D. Shankar, V. V. Gopalakrishna, S. S. C. Shenoi, F. Durand, S. R. Shetye, N. Araligidad, and G. S. Michael, Physical Oceanography Division, National Institute of Oceanography, Dona Paula, Goa 403004, India (shankar@darya.nio.org).

C. K. Rajan and Z. Johnson, Department of Atmospheric Science, Cochin University of Science and Technology, Kochi 682016, India.

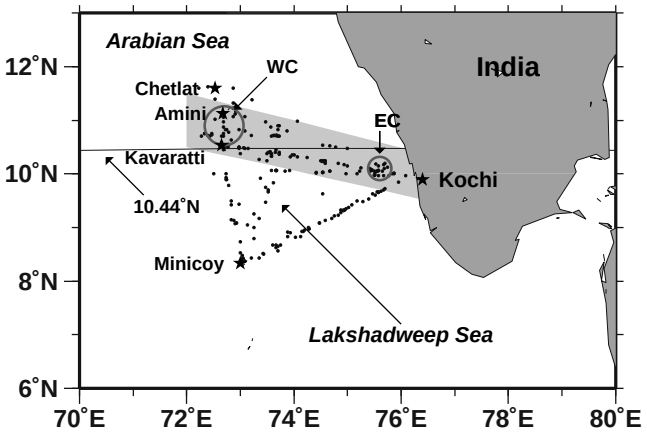

Figure 1. The region of the XBT surveys was the Lakshadweep Sea. The ships used for the XBT surveys are feeder ships for the islands in the Lakshadweep chain. Some of these islands are marked by asterisks. The location of all the XBT profiles and surface salinity samples collected during May-2002–April-2003 is marked by dots. The best sampled track, shown by the light gray shading, runs between Kochi and the islands in the northwestern LS (Kavaratti, Amini, and Chetlat among them). The inversions marked on the time-longitude plots in Figure 3b,c are from this track and they are superimposed on the model temperature inversion and surface salinity along the 10.44°N section, which bisects the track. The model results for the latitude range of the shaded XBT track are almost identical, the difference being the slight decrease in Rossby wave speed towards the north. The time-depth sections in Figure 3d,e and the surface salinity data in Figure 3f are for the two circles marked EC (Eastern Circle) and WC (Western Circle), which lie near the ends of the best-sampled track.

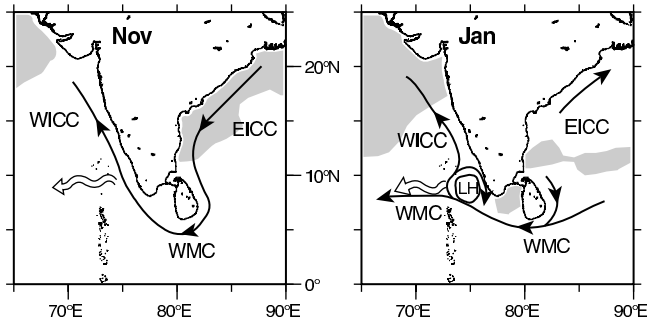

Figure 2. Schematic showing the evolution of the circulation in the LS. The acronyms are as follows: EICC, East India Coastal Current; WMC, Winter Monsoon Current; WICC, West India Coastal Current; and LH, Lakshadweep (sea-level) high. In November (left), the EICC feeds into the WICC through the WMC south of India. The westward radiation of Rossby waves, depicted by the wiggly arrow, leads to the formation of the LH by January (right). The shaded areas are the regions where the net flux is out of the ocean.

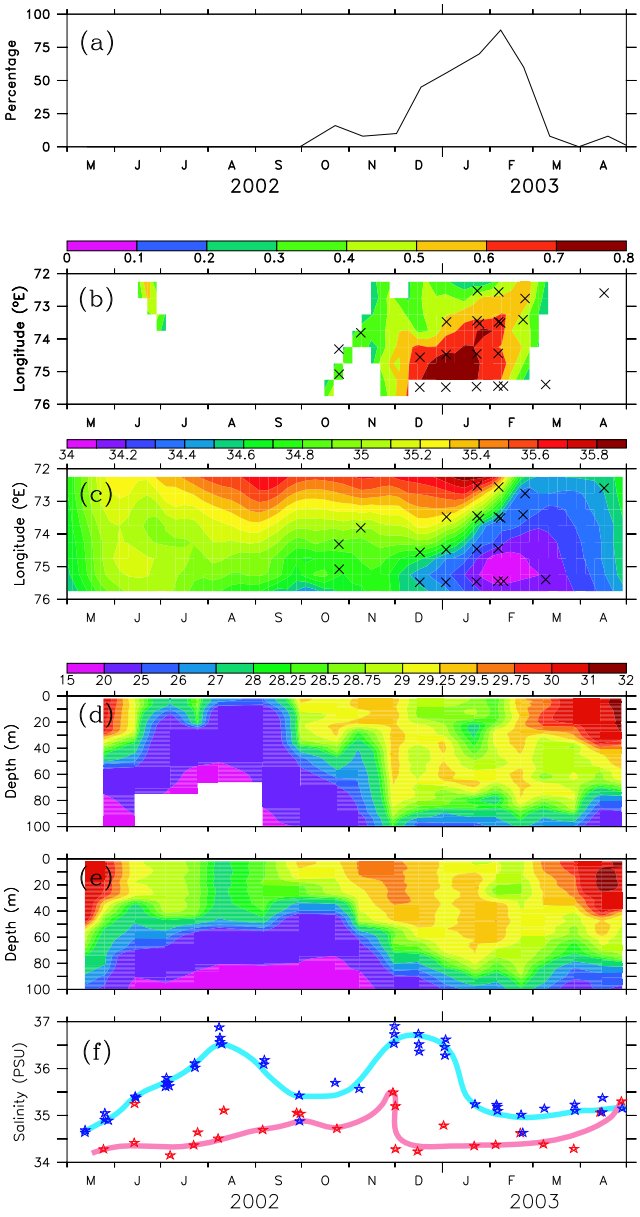

Figure 3. The evolution of temperature inversions and surface salinity in the LS. **(a)** Percentage of profiles (for the entire LS) that show inversions during each voyage. 7–13 XBTs were launched per voyage, but this variation in sampling does not affect the observed variation in occurrence of inversions. **(b)** Time (abscissa)– longitude (ordinate) plot of temperature inversion (°C) along 10.44°N from the climatological model simulation of *Durand et al.* [2004]. The colour gives the magnitude of temperature inversion; absence of colour indicates absence of inversion. The crosses superimposed on the model field mark the locations where temperature inversions occur in the XBT data along the best-sampled track between Kochi and the northwestern LS; the model section bisects this track (see Figure 1). Note that the model simulation is a climatology, but the data are for 2002–2003. **(c)** As in (b), but the colour is for model surface salinity (PSU). **(d)** Time-depth plot of XBT temperature, smoothed with a 5-point running mean, for the eastern LS (eastern circle in Figure 1). Note that the scale, common to (d) and (e), is not uniform. **(e)** As in (d), but for the western LS (western circle in Figure 1). **(f)** Observed surface salinity (PSU) for the eastern (red) and western (blue) circles in Figure 1. Note that salinity decreases sharply in end-November in the eastern circle and in end-December in the western circle.